

## Electronic Supporting Information

### **Synthesis of interface-modulated ultrathin Ni(II) MOF/g-C<sub>3</sub>N<sub>4</sub> heterojunctions as efficient photocatalysts for CO<sub>2</sub> reduction**

Lina Zhao,<sup>a,b</sup> Zhenlong Zhao,<sup>a</sup> Yuxin Li,<sup>\*a</sup> Xiaoyu Chu,<sup>a,b</sup> Zhijun Li,<sup>a</sup>

Yang Qu,<sup>a</sup> Linlu Bai,<sup>\*a</sup> and Liqiang Jing<sup>\*a</sup>

<sup>a</sup>Key Laboratory of Functional Inorganic Materials Chemistry (Ministry of Education), School of Chemistry and Materials Science, International Joint Research Center and Lab for Catalytic Technology, Heilongjiang University, Harbin 150080, P. R. China.

<sup>b</sup>Department of Food & Environmental Engineering, East University of Heilongjiang, Harbin 150066, P. R. China.

## Figures

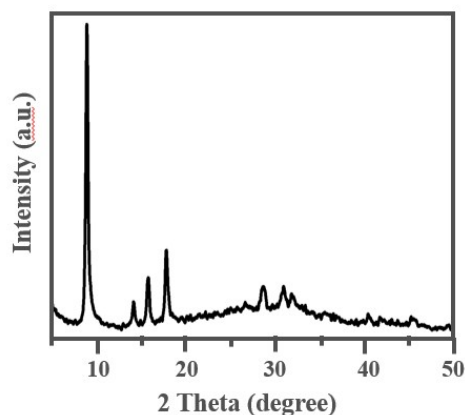


Figure S1. PXRD pattern of NiMOF nanosheets prepared in a control experiment

Note: The ultrathin NiMOF nanosheet was prepared as following. First, DMF (32 ml), ethanol (2 ml) and water (2 ml) were mixed in a 100 ml flash bottle. Next, 0.75 mmol BDC was dissolved into the mixed solution under ultrasonication. Subsequently, 0.75 mmol  $\text{NiCl}_2 \cdot 6\text{H}_2\text{O}$  were added. After  $\text{Ni}^{2+}$  salts were dissolved, 0.8 ml TEA was quickly injected into the solution. Then, the solution was stirred for 5 min to obtain a uniform colloidal suspension. Afterwards, the colloidal solution was continuously ultrasonicated for 8 h (40 kHz) under airtight conditions. Finally, the products were obtained via centrifugation, washed with ethanol (3~5 times), and then freeze drying.

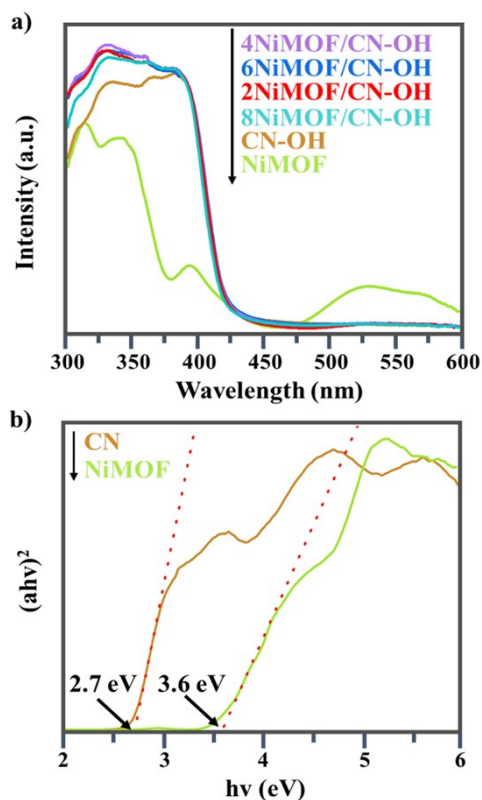


Figure S2. The UV-vis DRS spectra of NiMOF, CN-OH and NiMOF/CN-OH with a proper amount of NiMOF (a). Tauc plots of CN and NiMOF for bandgap calculation based on UV-vis DRS spectra (b).

Note: The optical bandgap is determined from the UV-vis DRS spectra by following the equation proposed by Tauc, Davis, and Mott:  $(ah\nu)^{1/n} = A(h\nu - E_g)$ , where  $a$  stands for the absorption coefficient,  $h$  is Planck's constant,  $\nu$  represents the frequency of vibration,  $E_g$  is the bandgap,  $A$  expresses the proportional constant, and  $n$  denotes the nature of the sample transition. As  $(ah\nu)^{1/n}$  is plotted against  $h\nu$ , a distinct linear regime can be obtained, which denotes the onset of the absorption. By extrapolating the linear region to the abscissa, the energy for the optical bandgap of the material will be yielded.

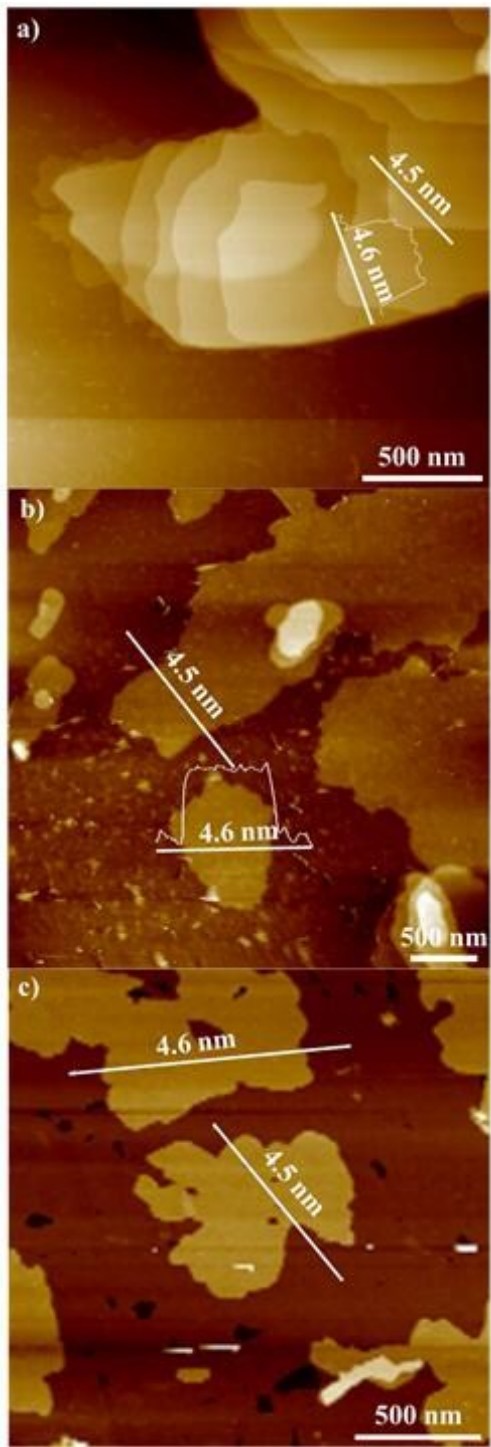


Figure S3. AFM images and height data of CN (a), CN-OH (b) and CN-AA (c).

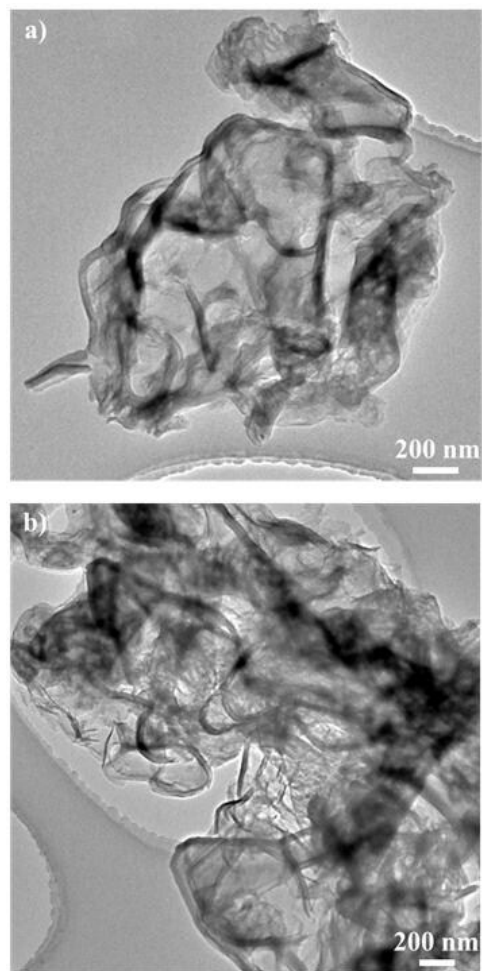


Figure S4. The TEM images of CN-OH (a) and CN-AA (b).

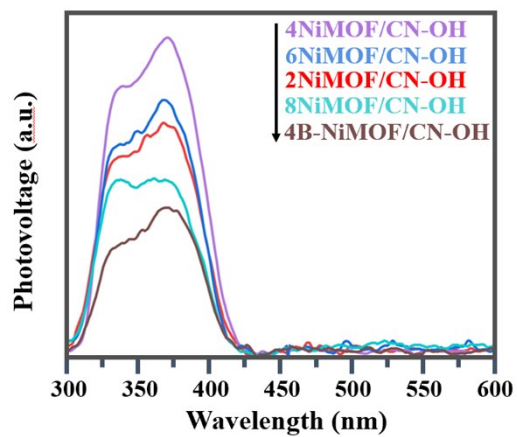


Figure S5. SS-SPS spectra of NiMOF/CN-OH with a proper amount of ultrathin or bulk NiMOF.

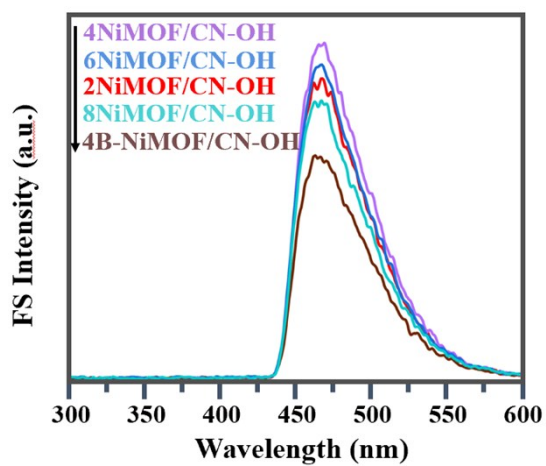


Figure S6. FS spectra related to the amount of produced  $\cdot\text{OH}$  for NiMOF/CN-OH with a proper amount of ultrathin or bulk NiMOF.

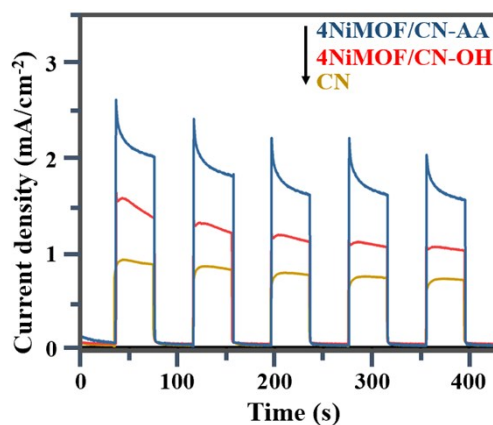


Figure S7. The transient photocurrent-time curves of CN, 4NiMOF/CN-OH and 4NiMOF/CN-AA.

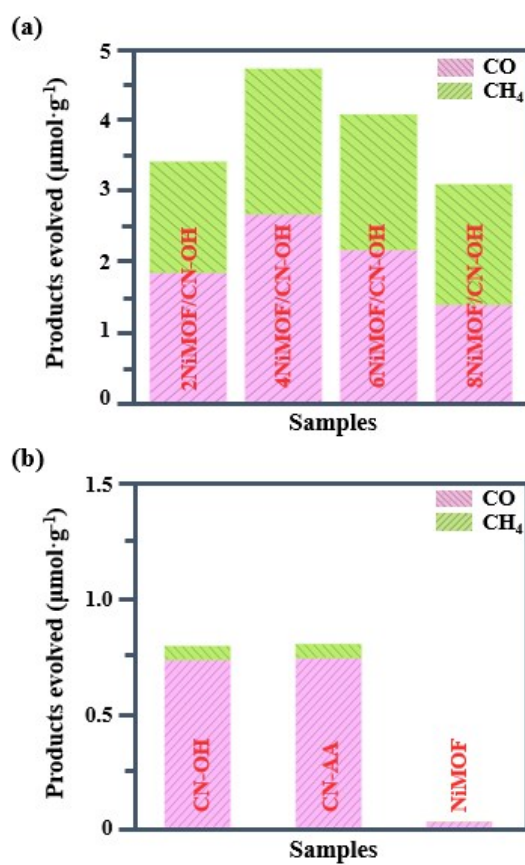


Figure S8. Photocatalytic activities for CO<sub>2</sub> conversion under visible-light irradiation for 4 hours of NiMOF/CN-OH with a proper amount of NiMOF (a) and for 4 hours of NiMOF, CN-OH and CN-AA (b).

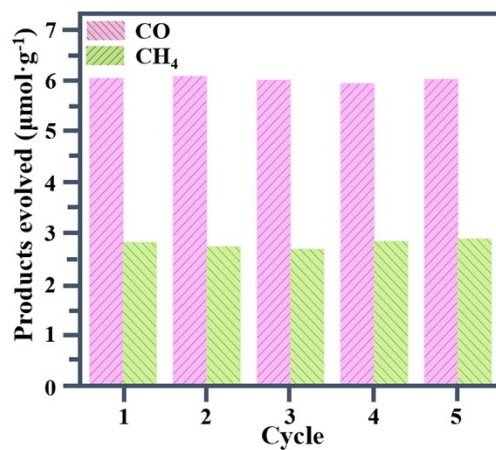


Figure S9. Stability test on visible-light photocatalytic activities for CO<sub>2</sub> reduction of 4NiMOF/CN-AA for 5 cycles.

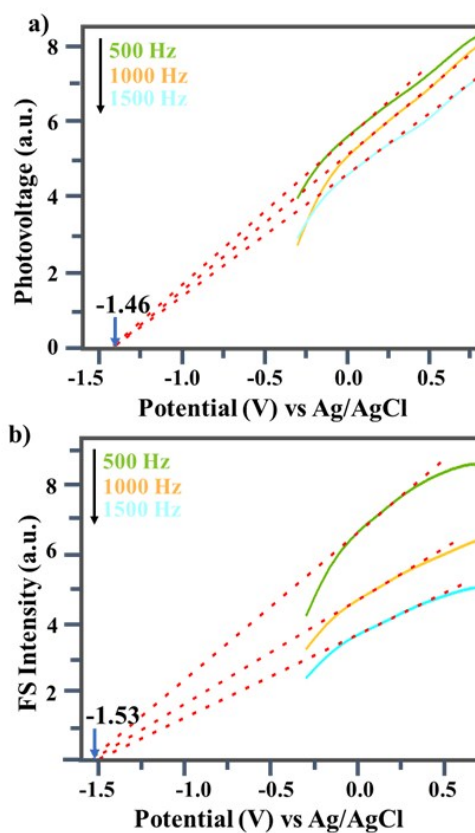


Figure S10. The Mott-Schottky spectra of CN (a) and NiMOF (b). The flat-band potential is determined from the Mott-Schottky plot, and is approximately equal to the intercept on the x-axis of the tangent to the inflection point of the C<sup>2</sup>-E curve.

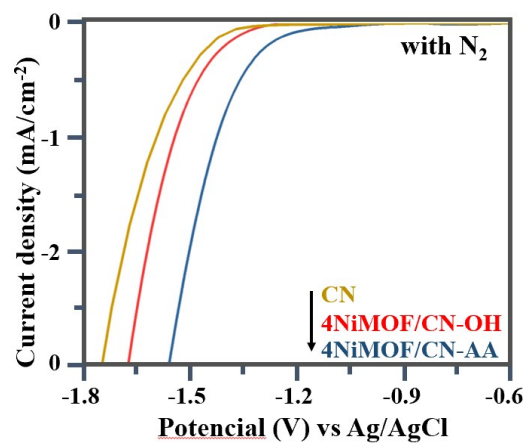


Figure S11. Electrochemical reduction spectra of CN, 4NiMOF/CN-OH and 4NiMOF/CN-AA under N<sub>2</sub> bubbled system.

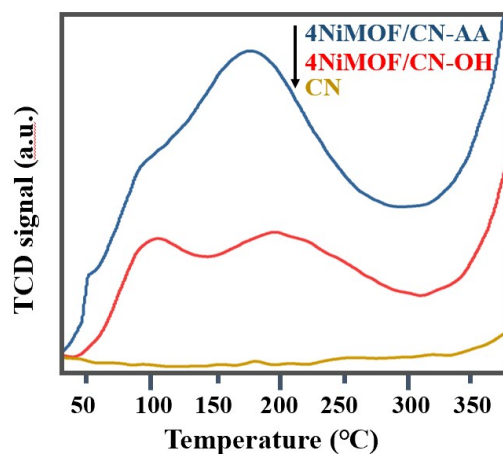


Figure S12. CO<sub>2</sub> TPD spectra of CN, 4NiMOF/CN-OH and 4NiMOF/CN-AA.

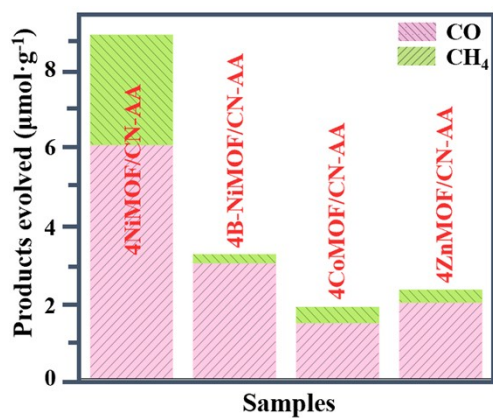


Figure S13. Photocatalytic activities for CO<sub>2</sub> conversion under visible-light irradiation for 4 hours of 4NiMOF/CN-AA, 4B-NiMOF/CN-AA, 4CoMOF/CN-AA and 4ZnMOF/CN-AA.

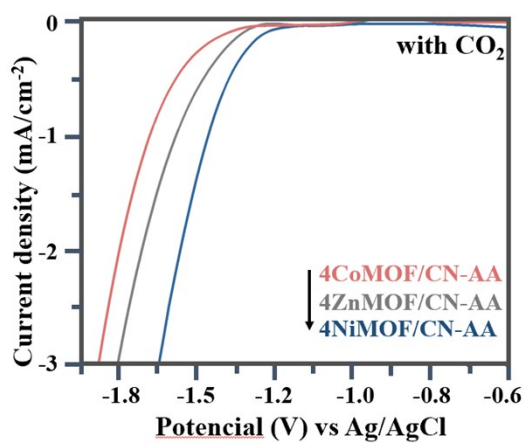


Figure S14. Electrochemical reduction spectra of 4NiMOF/CN-AA, 4ZnMOF/CN-AA and 4CoMOF/CN-AA under CO<sub>2</sub> bubbled system.

Table S1. Comparison on activities of MOF/CN-based heterojunction photocatalysts for CO<sub>2</sub> conversion in the publications and this work.

Photocatalyst	Solvent	Light resource	Major products and improvement	References
UiO-66/CNNS (10 wt% carbon nitride)	triethanolamine (TEOA) and acetonitrile (MeCN)	300 W Xe-lamp	3-fold (CO)	<i>Ref. 23</i>
TCNZ8	NaHCO <sub>3</sub> (84 mg.) and H <sub>2</sub> SO <sub>4</sub> aqueous solution (0.3 mL, 2 M)	300 W Xe-lamp	3-fold (CH <sub>3</sub> OH)	<i>Ref. 24</i>
BIF-20@g-C <sub>3</sub> N <sub>4</sub>	MeCN/TEOA = 4:1	300 W Xe-lamp	9.7-fold (CH <sub>4</sub> ) 9.85-fold (CO)	<i>Ref. 25</i>
NUZ/HGN-35%	H <sub>2</sub> O/TEOA = 20:1	300 W Xe-lamp	3-fold (CO)	<i>Ref. 26</i>
4NiMOF/CN-AA	H <sub>2</sub> O	300 W Xe-lamp	18-fold (CH <sub>4</sub> +CO)	Our work